

# Retrieval of Cirrus Cloud Properties from Split Window and 6.7 $\mu\text{m}$ Measurements (I')

T. Inoue and Y. Mano  
 Meteorological Research Institute / JMA  
 1-1 Nagamine Tsukuba, Ibaraki 305, Japan

## Introduction

A major uncertainty in our present understanding of the climate system is the effect of clouds. Among these, cirrus clouds play an especially important role in the global climate system. Since Manabe and Stricker (1964) studied the effect of clouds on the radiation budget, cirrus clouds have been seen as having a "greenhouse" effect on the atmosphere. However, the radiative properties of these clouds are little known due to the difficulty of direct observation.

Satellite remote sensing is considered an effective tool for observing cirrus cloud radiative properties, but the clouds are difficult to detect. Thus far, the number of cirrus cloud detection algorithms using satellite observations is very small. Single-channel infrared methods are of limited utility due to the semi-transparency of many cirrus. Other investigators use visible and 3.7  $\mu\text{m}$  data; however, these algorithms cannot be used equally during both day and night.

Inoue (1985) first demonstrated the usage of split window data (11  $\mu\text{m}$  and 12  $\mu\text{m}$  in combination), which can be used equally both day and night, in detecting cirrus clouds. Some theoretical and observational studies to use the split window in retrieving cirrus cloud properties were followed (e.g., Wu [1987], Prabhakara et al. [1988], Parol et al. [1991], King et al. [1992]). The use of 6.7  $\mu\text{m}$  and 11  $\mu\text{m}$  for the study of semi-transparent clouds was first proposed by Szejwach (1982) and was followed by some works (e.g., Pollinger and Wendling [1984], Schmetz et al. [1993]). These two channels are effective in retrieving cirrus cloud temperature.

In this study, an algorithm to retrieve optical thickness and effective radius of cirrus clouds using split window data and 6.7  $\mu\text{m}$  has been developed and applied to GOES-9 observations. The advantage of using these three channels is equal quality in retrievals for both day and night. In the near future, all geostationary meteorological satellites will carry the three channels, although current Geostationary Operational Environmental Satellites (GOES) and geostationary meteorological satellites (GMS) have these channels.

## Algorithm

Simulated brightness temperatures are computed from the radiative transfer equation for given optical thickness and cirrus cloud temperatures. Vertical temperature and water vapor profiles are taken from the U.S. standard tropical atmosphere. Cloud droplets are assumed to be spherical ice, and drop sizes are characterized by modified gamma distribution. Complex indices by Warren (1984) are used. Fluxes are computed by the 8-stream method. In this study, radiance for the split window is computed at 10.7  $\mu\text{m}$  and 11.8  $\mu\text{m}$ .

Figures 1a and 1b show computed brightness temperatures (TBB) and brightness temperature differences {BTD = TBB (10.7  $\mu\text{m}$ ) - TBB(11.8  $\mu\text{m}$ )} for effective radii of 10  $\mu\text{m}$  and 20  $\mu\text{m}$ , respectively. In this computation, water vapor absorption was neglected. These figures indicate the large BTD dependence on effective radius, but also show the possibility of retrieving cloud properties using TBB and BTD by assuming one parameter of either optical thickness, cloud

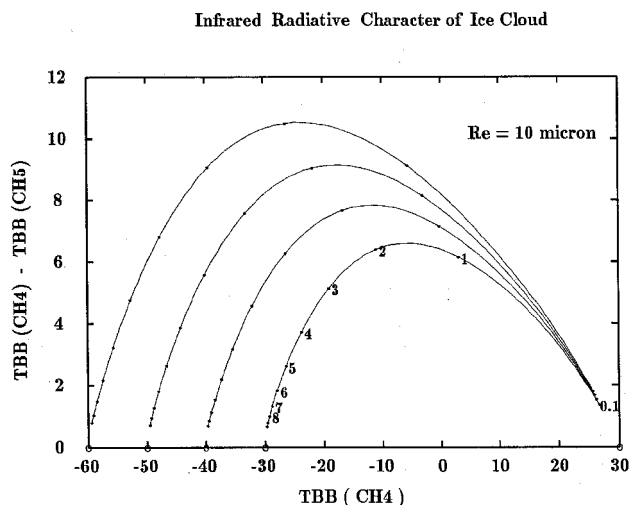
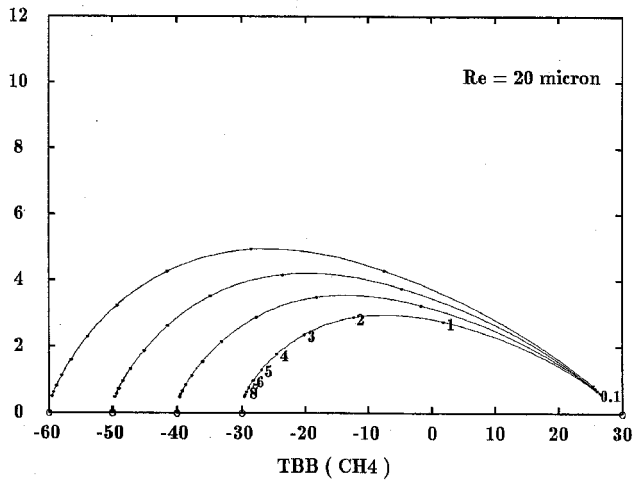


Figure 1a. Computed TBB and BTD for effective radius of 10  $\mu\text{m}$  for different cirrus cloud temperatures.

Infrared Radiative Character of Ice Cloud



**Figure 1b.** Computed TBB and BTB for effective radius of 20  $\mu\text{m}$  for different cirrus cloud temperatures.

temperature, or effective cloud radius. The International Satellite Land Surface Climatology Project (ISCCP) assumes the effective radius, while Kuwahara et al. (private communication) assume cloud height. In this study, cirrus cloud temperatures are estimated from 11  $\mu\text{m}$  and 6.7  $\mu\text{m}$  observations. Figure 1c shows BTB as a function of effective radius and optical thickness when cirrus cloud temperature fixes at  $-50^\circ\text{C}$ .

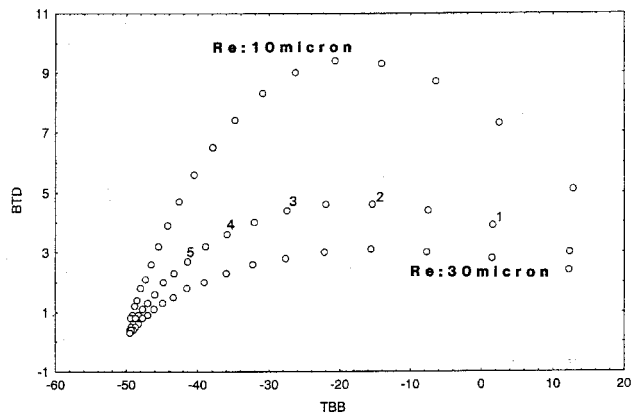


**Figure 1c.** TBB and BTB as a function of effective radius and optical thickness when cirrus cloud temperature fixes at  $-50^\circ\text{C}$ .

The table of TBB and BTB is constructed in advance for various cloud temperatures, optical thickness, effective radii, and satellite zenith angles using the standard tropical

atmosphere or global analysis data from the Japan Meteorological Agency (JMA). Actual TBB and BTB are used to find an optimal optical thickness and effective radius.

## Data

This study uses utilizes split window data and 6.7  $\mu\text{m}$  data observed by GOES-9. GOES-9 data were acquired by the McIDAS (Man computer Interactive Data Access System) at MRI/JMA. The 8-km spatial resolution with 10 bits data are processed.

## Cirrus Cloud Temperature Retrieval from 11 $\mu\text{m}$ and 6.7 $\mu\text{m}$

Based on the idea of Szejwach (1982), linearity of radiance at 11  $\mu\text{m}$  and 6.7  $\mu\text{m}$  is studied for cirrus clouds over the central Pacific. Figures 2a and 2b show examples of scatter

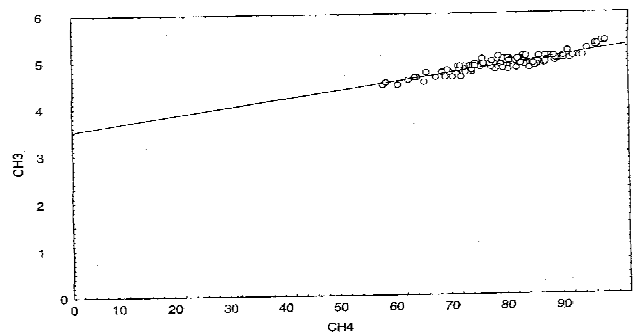


**Figure 2a.** Scatter plot of 11  $\mu\text{m}$  and 6.7  $\mu\text{m}$  radiances for cirrus anvil.

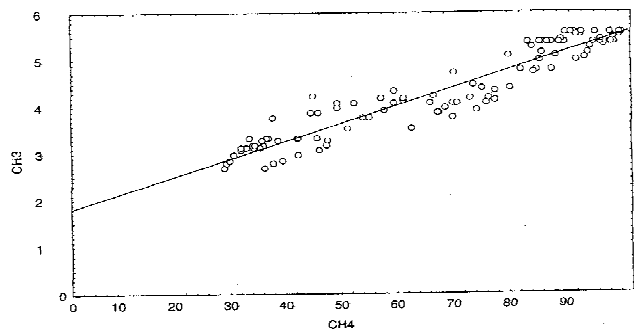


**Figure 2b.** Scatter plot of 11  $\mu\text{m}$  and 6.7  $\mu\text{m}$  radiances for different cirrus anvil.

plots of 11  $\mu\text{m}$  and 6.7  $\mu\text{m}$  radiance for cirrus anvils associated with deep convection. Cirrus cloud pixels of 10 by 10,

which belong to the same anvil selected by subjective inspection of the BTD image, are used to construct the plots.

Generally, we can see good linearity between the two radiances for cirrus clouds. The bold curve in Figure 3 (similar scatter plot for another group of cirrus clouds) corresponds to a black-body cloud. Cirrus cloud temperature can be estimated from the intersection of the bold curve and the regression line for cirrus clouds. In this method, cirrus cloud temperature is determined for a group of cirrus cloud pixels (e.g., 10 by 10), although two pixels are enough to fit the line. We found that derived cloud temperatures reasonably agree with the TBBs for the central region of the convection.

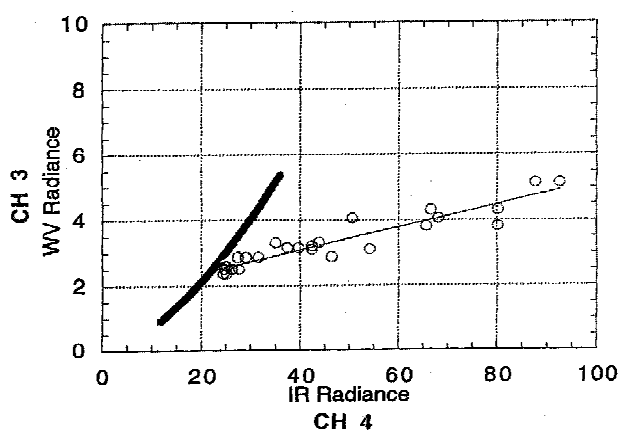


**Figure 3.** Scatter plot of 11  $\mu\text{m}$  and 6.7  $\mu\text{m}$  radiances for cirrus anvil.

## Results

Once cirrus cloud temperature is determined, the prepared tables of TBB and BTD are used to retrieve optical thickness and effective radius, pixel by pixel, for the group of cirrus clouds. Tables 1 through 3 show the retrieval results by the split window method. Each table shows the results for pixels from north to south (from top to bottom), where the convection core exists. Cloud temperature, which is estimated from 11  $\mu\text{m}$  and 6.7  $\mu\text{m}$  data, is assumed to be the same for each pixel in the same cirrus group. Retrieved optical thickness decreases with an increase in distance from the core of deep convection. The retrieved effective radius also decreases with the increase in distance from the center of convection. This finding is consistent with Kuwahara et al. (private communication), who indicate a positive correlation between optical thickness and effective radius.

**Table 1.** Retrieval Results Case 1.

Optical Thickness	Effective Radius	TBB 11 $\mu\text{m}$	TBB 12 $\mu\text{m}$
0.7	10	277.9	271.5
1.4	20	263.3	257.7
1.6	20	259.1	253.9
1.7	20	256.8	251.3
2.3	20	248.9	242.5
3.7	20	234.3	230.0
4.6	30	228.0	225.7

**Table 2.** Retrieval Results Case 2.

Optical Thickness	Effective Radius	TBB 11 $\mu\text{m}$	TBB 12 $\mu\text{m}$
0.3	10	289.8	284.8
0.4	10	286.2	280.1
0.7	10	277.7	270.4
1.5	20	259.3	252.3
2.5	20	241.3	234.7
3.1	20	233.0	227.4
3.9	30	226.3	222.4

**Table 3.** Retrieval Results Case 3.

Optical Thickness	Effective Radius	TBB 11 $\mu\text{m}$	TBB 12 $\mu\text{m}$
0.6	10	279.7	275.1
0.65	15	277.1	270.5
0.9	20	272.9	267.1
1.0	15	270.6	264.1
1.1	20	267.2	260.7
1.9	20	249.9	240.7
2.9	30	234.7	231.6
3.0	30	233.5	230.5

## Summary

A method of retrieving cirrus cloud optical thickness and mean effective radius and cloud temperature using three infrared data of split window and 6.7  $\mu\text{m}$  has been developed and applied to GOES-9 split window data. First, cloud temperature was estimated from 11  $\mu\text{m}$  and 6.7  $\mu\text{m}$  data, the optical thickness and effective radius were retrieved from split window. Case studies show reasonable cirrus cloud temperatures, which coincide with the temperature at the core of deep convection. Preliminary results for cirrus anvil associated with the deep convection show that retrieved optical thickness and mean effective radii become smaller as distance increases from the core.

In this study, spherical ice is assumed, and scattering in these wavelengths is neglected. Further study is required to assess the shape and scattering effects.

## References

- Inoue, T., 1985: On the temperature and effective emissivity determination of semitransparent cirrus clouds by bispectral measurements in the 10  $\mu\text{m}$  window region. *J. Meteor. Soc. Japan*, **63**, 88-98.
- King, M. D., Y. J. Kaufman, W. P. Menzel, and D. Tanr, 1992: Remote sensing of cloud, aerosol and water vapor properties from Moderate Resolution Imaging Spectrometer (MODIS). *IEEE Trans. Geoscience and Remote Sensing*, **30**, 2-27.
- Manabe, S., and R. F. Strickler, 1964: Thermal equilibrium of the atmosphere with a convective adjustment. *J. Atmos. Sci.*, **21**, 361-385.
- Parol, F., J. C. Buriez, G. Brogniez, and Y. Fouquart, 1991: Information content of AVHRR channels 4 and 5 with respect to the effective radius of cirrus cloud particles. *J. Appl. Meteor.*, **30**, 973-984.
- Pollinger, W., and P. Wendling, 1984: A bispectral method for the height determination of optically thin ice clouds., *Contrib. Atmos. Phys.*, **57**, 269-281.
- Prabhakara, C., R. S. Fraser, G. Dalu, M.L.C. Wu, R. J. Curran, and T. Styles, 1988: Thin cirrus clouds: Seasonal distribution over oceans deduced from Nimbus-4 IRIS. *J. Appl. Meteor.*, **27**, 379-399.
- Schmetz, J., K. Holmlund, J. Hoffman, B. Strauss, B. Mason, V. Gaertner, A. Koch, and L.V.D. Berg, 1993: Operational cloud-motion winds from Meteosat infrared images. *J. Appl. Meteor.*, **32**, 1206-1225.
- Szejwach, G., 1982: Determination of semi-transparent cirrus cloud temperature from infrared radiances: Application to METEOSAT. *J. Appl. Meteor.*, **21**, 384-393.
- Warren, S. G., 1984: Optical constants of ice from the ultraviolet to the microwave. *Appl. Opt.*, **23**, 1206-1225.
- Wu, M. C., 1987: A method of remote sensing the emissivity, fractional cloud cover, and cloud top temperature of high-level thin clouds. *J. Climate Appl. Meteor.*, **26**, 225-233.